



## **PRACTICAL ASPECTS OF ENGINEERING SEISMIC DAM SAFETY – CASE STUDY OF A CONCRETE GRAVITY DAM**

**David J. DOWDELL<sup>1</sup> and Benedict H. FAN<sup>2</sup>**

### **SUMMARY**

This paper reports on the practical issues encountered in the seismic assessment of a concrete gravity dam. Ruskin Dam is situated on a site for which the maximum design earthquake has a peak ground acceleration of 0.54g, corresponding to an annual probability of exceedance of  $10^{-4}$ . In the Ruskin dam deficiency investigations, a combination of 3-D and 2-D analyses, linear and non-linear, pseudostatic and dynamic, were employed in an attempt to bring together information necessary to form a seismic assessment of the dam and its appurtenant structures. A number of key parameters were investigated. These include: (1) selection of the appropriate damping level for use in assessing the structural response; (2) evaluation of the loads experienced by the upper portions of the dam and their variation along the dam due to the nature of the amplification of the of the seismic motion through the structure; (3) evaluation of the ability of the structure to develop 3-D action through the grouted shear keys at contraction joints between monoliths; (4) evaluation of the hydrodynamic loads on the spillway gates considering the interaction between the dam and the gates. From these experiences, the need for research in critical areas is indicated.

### **INTRODUCTION**

Completed in 1930, the Ruskin Dam is a 58m tall concrete gravity dam, located on the Stave River system, a tributary of the Fraser River approximately 55km east of Vancouver. The dam impounds the Hayward Lake reservoir, having a surface area of 2.98 km<sup>2</sup> at the maximum normal operating level. This relatively small reservoir is fed by the outflow from the much larger Stave Lake reservoir 6 km upstream, which is retained by the older Stave Falls Dams. Outflow from the Ruskin project enter the lower reaches of the Stave River approximately 2 km upstream of its confluence with the Fraser River.

The dam, pictured in Figure 1, and illustrated in Figure 2, is a concrete gravity structure situated in a narrow valley. The dam is founded on rock. The dam is 130m long at the road deck, comprising a 7-bay radial-gated spillway section 85m long and non-overflow sections on either side. The spillway gates each

---

<sup>1</sup> Senior Engineer, BC Hydro Engineering, Burnaby, Canada. Email: dave.dowdell@bchydro.com

<sup>2</sup> Principal Engineer, BC Hydro Engineering, Burnaby, Canada. Email: ben.fan@bchydro.bc.ca



**Figure 1 – Photograph of Ruskin Dam Looking NE**

measure 10m wide by 8m high. Spillway piers support a single lane roadway at the top of the dam. Figure 2 provides Y-dir chainages and Z-dir elevations in both traditional Imperial units and S.I. units. Elevations in traditional Imperial units do not have the same datum as those expressed in S.I. units.

The abutment rock at the right rises to a local maximum about 15 m below the top of the dam and dips away from the structure. The rock on the left abutment rises above the top of the dam but also dips away from the structure further to the east. The seismic withstand of the natural soils retaining the reservoir on both abutments is an important consideration. Gate operability requirement for reservoir control following a large earthquake is closely linked to the risk reduction of potential seepage and erosion in the abutment soils.

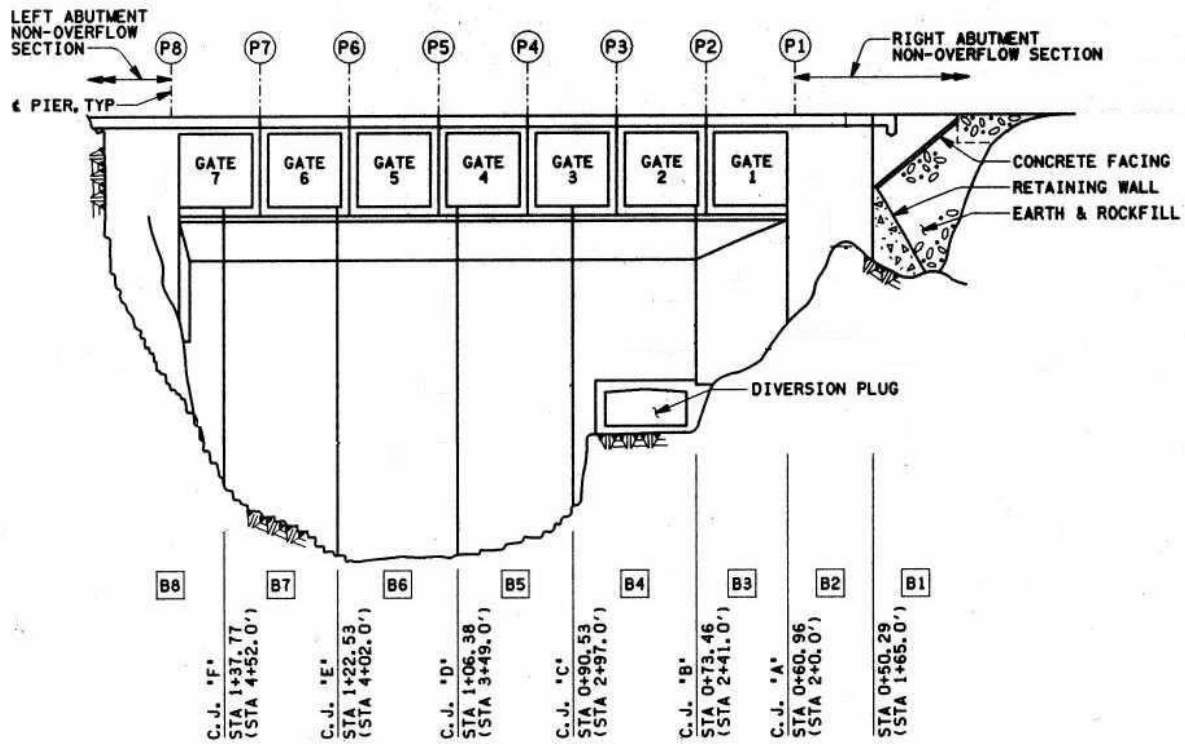
The site seismic design parameters used in the assessment of the structure is illustrated by the curves in Figure 3. The design basis earthquake (DBE) peak ground acceleration PGA corresponding to an annual probability of exceedance of  $2.1 \times 10^{-2}$  is 0.23g, and the PGA for the maximum design earthquake (MDE) is 0.54g for an annual exceedance probability of  $1 \times 10^{-4}$ . The peaks of the associated response spectra are 0.56g for the DBE and 1.27g for the MDE.

The dam was designed to take advantage of the narrow valley. Adjacent monoliths are keyed at the contraction joints, which were grouted after initial construction. There is some evidence that vertical steps were provided to enhance the ability of the lift joints to carry shears across the horizontal plane. A typical vertical section and shear key detail is shown in Figure 4.

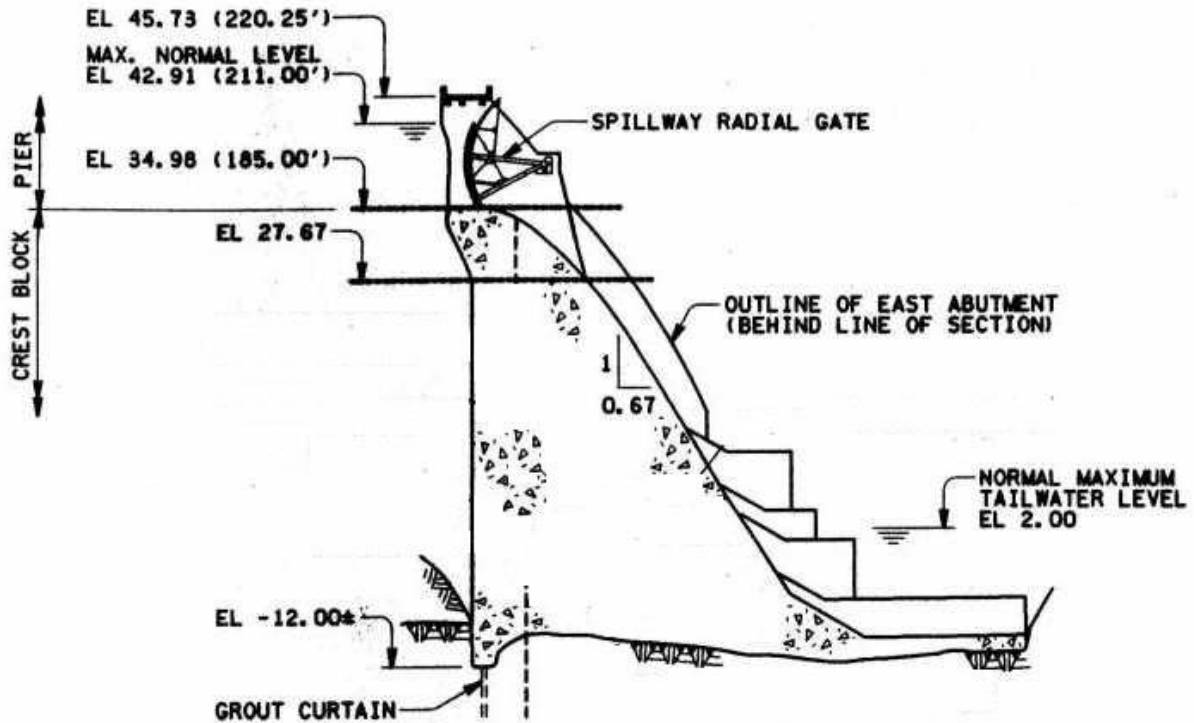
Overall, the dam is in good condition. Concrete cores extracted from the body of the dam were tested in unconfined axial compression and in unconfined shear and the strength values indicate average strengths of 27 MPa in compression and 4.6 MPa in shear.

The objective of the deficiency investigation project was to assess the seismic demands on the structure, its ability to meet these demands and, where necessary, develop conceptual upgrade alternatives. The items under consideration included the body of the dam, the piers and the gates. During the course of the investigation, several issues arose:

- (1) Selection of the appropriate level of damping to be used in assessing the dam response



(a) Upstream Elevation



(b) Vertical Section

Figure 2 – Elevation and typical section of Ruskin Dam. Elevations are given in S.I. as well as Imperial units. Note that S.I. unit elevations have a different datum than those given in Imperial.

- (2) Evaluation of the loads experienced by the upper portions of the dam due to varying degrees of amplification of the seismic motion
- (3) Evaluation of the ability to develop 3-D action through existing shear keys and the extent of load transfer between adjacent dam blocks
- (4) Evaluation of the hydrodynamic loads on the gates considering the interaction between the gates and the dam

In this paper the methods used to evaluate the above items are described.

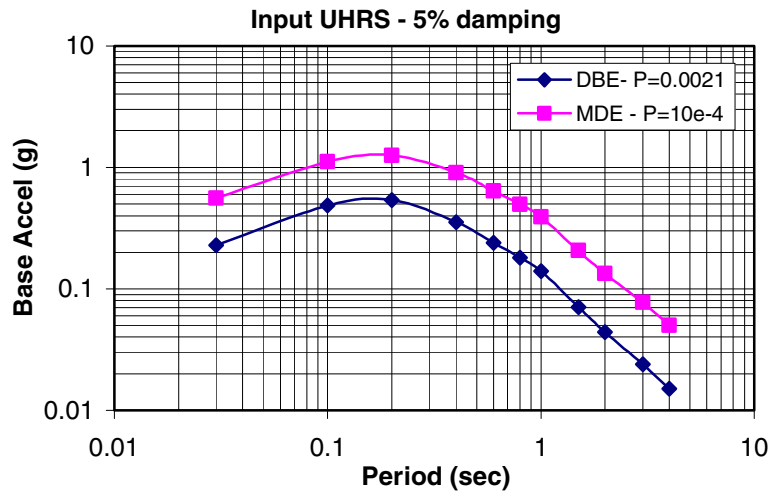


Figure 3 – UHRS MDE and DBE response spectra (5% damping)

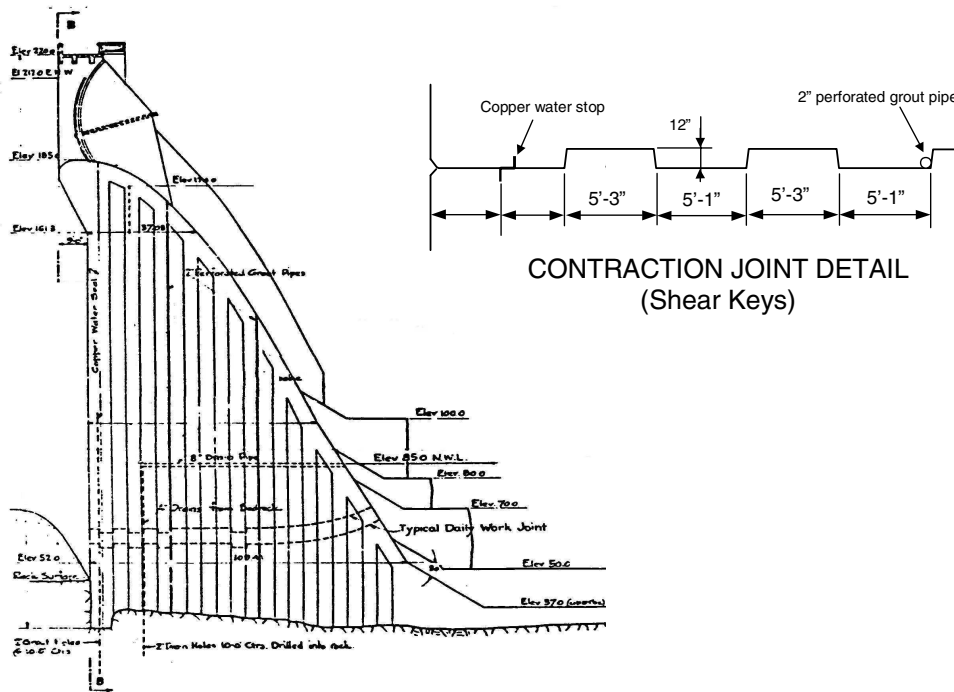


Figure 4 – Shear key locations and dimensions

## DAMPING STUDY

Selection of the appropriate damping level is an important consideration as it inversely affects the magnitude of the loads that the dam and its components experience during earthquakes. Chopra and Tan [1], as part of the simplified method for the evaluation of the spillway monoliths provide the following formula for the evaluation of overall system damping,  $\xi$ , taking interactions of the dam-foundation-reservoir system into account:

$$\xi = \frac{1}{R_r} \frac{1}{(R_f)^3} (\xi_1 + \xi_r + \xi_f) \quad (1)$$

where  $\xi_1$ ,  $\xi_r$  and  $\xi_f$  represent the fundamental mode damping of the structure, the incremental damping associated with the reservoir and the incremental damping associated with the foundation, respectively. The factors  $R_r$  and  $R_f$  represent frequency ratios associated with the presence of the reservoir and the compliance of the foundation as compared to the frequency of the structure itself on a rigid foundation. Using this relationship with estimated parameters for foundation modulus and concrete modulus yielded damping values ranging from 11%-23% of critical damping. Consistent with values determined using the formula above, Okamoto [2] observed values in the order of 10%-20% in structures subjected to large ground motions. In a survey paper covering worldwide dam experience, however, Hall [3] found damping ratios in the range of 2%-5% for a great many structures based in large part on shaker testing. It was the belief of the project team that the difference in the damping was due to the level of shaking, consistent with the discussion by Okamoto. The project team attempted to resolve this issue by initiating, an investigation of the level of damping observed in dam structures in actual earthquakes.

Two structures similar to Ruskin Dam that had experienced significant earthquakes were identified, Detroit Dam in Oregon and the Lower Crystal Springs Dam in California. The table below provides a comparison of these structures and Ruskin Dam. Both dams had recorded earthquake motions at the base and the crest of the structure such that damping estimates could be computed using the half power bandwidth method and the log decrement method. Many other structures have experienced significant earthquake motions, however, because of lack of instrumentation or failure of instruments, they could not be used.

**Table 1. Comparison of dams used in the damping study.**

Dam	Type	Crest Height (m)	Crest Length (m)	Earthquake	Base US/DS PHGA (g)
Detroit Dam	Conc Gravity	141	-	1993 Scotts Mills	0.026g
Lower Crystal Springs	Conc Gravity	42	183	1989 Loma Prieta	0.052g
Ruskin	Conc Gravity	58	130	MDE	0.54g

The half-power bandwidth uses the shape of the power spectral density (PSD) plot of the transfer function to estimate damping. The transfer function is determined by taking the ratio of the PSD's of the output response to the input excitation leaving only a representation of the frequency response of the structure. A lightly damped structure will exhibit a sharp high peak at the fundamental frequency of an excited mode, while a heavily damped structure will exhibit a low broad hump. With the log decrement method, the time history of vibration is observed during periods when the excitation is zero or very small. The rate of decay of vibrations, assumed to be in the dominant mode, is used to estimate the damping.

Carrying out these analyses with the available time histories led to the identification of relatively low damping values associated with identified modes, on the order of 1% of critical damping. It was also observed, that although the earthquakes produced significant motions in these structures, the level of motion was a factor of 20 lower than the MDE in the case of Detroit Dam and an order of magnitude less than the MDE in the case of Lower Crystal Springs. The overall conclusion of this study was that higher damping (beyond 5% of critical) in an undamaged (elastic) structure could not be supported with available data at this time.

## **DYNAMIC PROPERTIES AND AMPLIFICATIONS - FE MODEL OF THE DAM**

The finite element model, shown in Figure 5, was constructed using ANSYS to study the dynamic properties of the structure and the interaction between monoliths. It was constructed of simplified geometry using rectangular block and wedge-shaped 8 and 6-noded elements. The foundation was modelled as massless, having elastic moduli ranging from 6 GPa beneath the tallest monoliths to 30GPa on the abutments. These were consistent with a zone of sheared rock beneath the dam. Zangar hydrodynamic masses were attached to the nodes of the wetted portion of the upstream face. Static reservoir forces were applied at the upstream face nodes. Because of the coarseness of the model, it was not intended to use the analysis results to extract stresses. Rather, they were intended to be used to extract mode shapes and frequencies and the forces transferred between blocks.

Each of the 8 monoliths was rigidly connected to the foundation elements. Vertical interfaces between adjacent monoliths were treated in one of two ways: (1) with rigid connections such that the model would be monolithic and linear and (2) meshed with non-linear contact elements that enable the adjacent monoliths to transfer contact forces and tractions. The elastic model was used to perform linear response spectrum analysis in order to extract accelerations for subsequent pseudostatic analysis of the upper portions of the structure. The non-linear model was used in a pseudostatic analysis to estimate the levels of load transfer between adjacent monoliths. This was to account for the 3-D behaviour of the dam in its narrow valley and permit subsequent 2-D assessments to be performed with a greater degree of precision than possible using the 3-D model directly.

### **Linear FE Model – Modal Analysis**

The frequencies determined by the modal analysis of the linear ANSYS model are shown in Table 2. These are compared with the frequencies determined in a 1995 finite element study using a much more detailed (but linear and monolithic) model and with modes identified by Kemp *et al.* [4] through the analysis of ambient vibration data collected at points along the crest and within the body of the dam. A plot of the first mode shape is given in Figure 6.

**Table 2. Comparison of natural frequencies, current model and previous studies**

<b>Mode Shape</b>	<b>Current ANSYS model</b>	<b>1995 BCH ANSYS model</b>	<b>Kemp <i>et al.</i> ambient vibration study [4]</b>
1	6.7	7.5	7.1
2	9.4	11.6	12.5
3	11.3	-	13.3

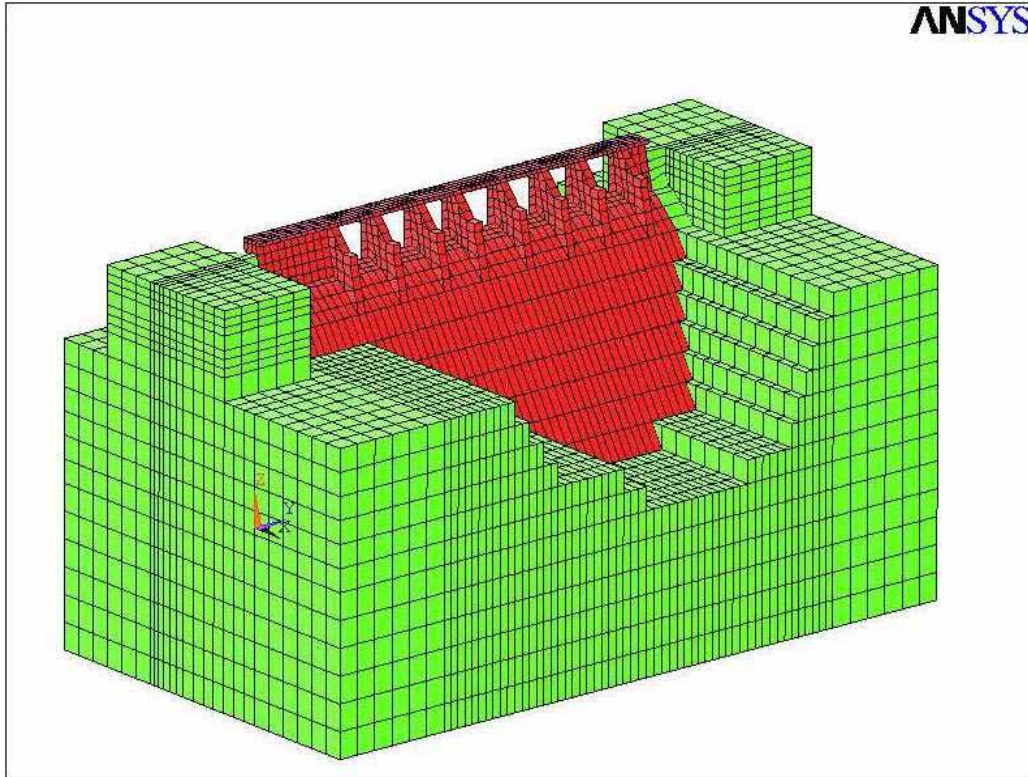


Figure 5 – ANSYS finite element model - Ruskin main concrete dam and foundation.

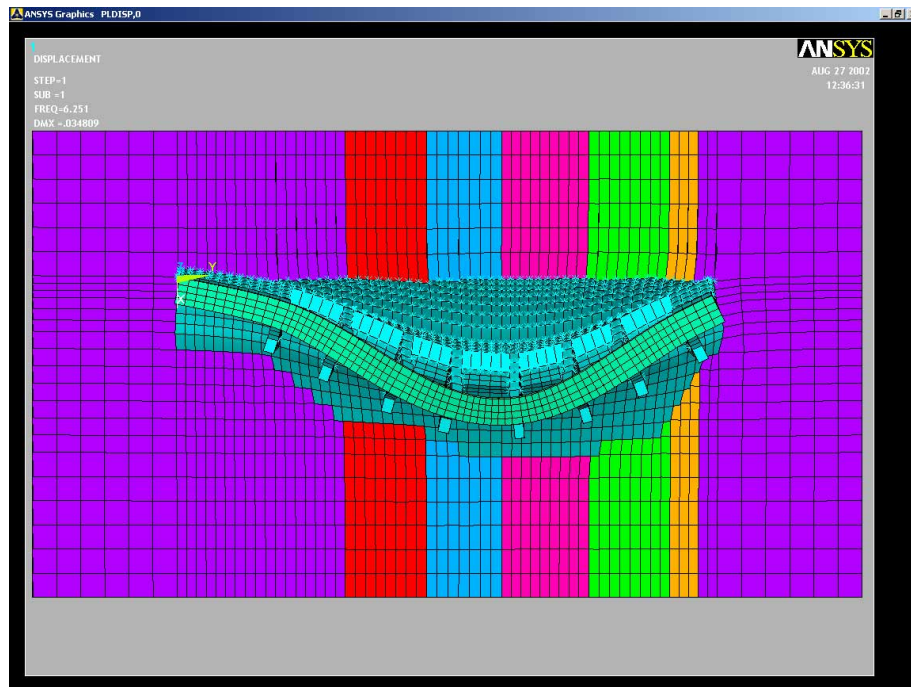


Figure 6 – Plan view ANSYS model fundamental mode shape (model without abutment rock restraint).

Examination of the ANSYS output confirmed that modal accelerations are computed relative to the fixed base. The relative coordinate acceleration results are not correct for computing inertial forces in pseudostatic analysis. In order to estimate accelerations with respect to the absolute co-ordinate system, the results obtained were corrected by performing a subsequent SRSS modal combination of the rigid body mode with peak response by definition equal to the peak ground acceleration as given by

$$a_{absolute}(x, y, z) = \sqrt{a_{relative}(x, y, z)^2 + PGA^2} \quad (2)$$

where the co-ordinates  $(x, y, z)$  indicate that this process is applied to all points of the structure. Amplifications were computed as the ratio of the absolute acceleration extracted at a point to the free field peak ground acceleration.

$$A(x, y, z) = \frac{a_{absolute}(x, y, z)}{PGA} \quad (3)$$

The amplifications were established at key points of interest, including the centroids of the piers above the spillway gate sill level and the centroids of the blocks above El. 27.67 m, termed the crest blocks. This procedure produced amplifications in the piers as shown in Table 3 below. The absolute co-ordinate corrected results were found not to differ significantly at these points from corresponding relative acceleration values due to the already high amplifications. Table 3 includes amplifications associated with 5%, 10% and 20% damped spectra to illustrate the significance of damping.

**Table 3. Amplification Factors – evaluated at chosen locations within Ruskin Dam. (See Fig. 2)**

Location		Co-ordinates			Amplification		
Section	Pos.	X (m)	Y (m)	Z (m)	$\xi=5\%$	$\xi=10\%$	$\xi=20\%$
Pier	P2	1.40	72.09	41.26	3.61	2.71	2.02
	P3	1.40	84.28	41.26	4.95	3.71	2.99
	P4	1.40	96.47	41.26	6.62	4.97	3.76
	P5	1.40	108.66	41.26	7.79	5.84	4.05
	P6	1.40	120.85	41.26	6.32	4.74	3.38
	P7	1.40	133.05	41.26	4.19	3.14	2.44
	Crest Block	B3	3.05	68.43	34.19	2.23	
B4		3.05	82.60	34.19	3.35		1.85
B5		3.05	97.99	34.19	4.50		2.31
B6		3.05	114.76	34.19	4.48		2.05
B7		3.05	130.61	34.19	3.14		1.66
B8		3.05	145.67	34.19	1.95		1.11

It is apparent that the amplifications vary significantly across the crest of the structure. The amplification for the most heavily loaded pier (P5) is more than twice that of the least loaded pier (P2).

#### **Non-linear ANSYS model - load sharing in the body of the Dam**

During prior seismic structural analyses performed in 1995, material strength test data was not available. At the time, using much more conservative shear strength estimates led to the conclusion that the shear keys would likely fail and, consequently, each monolith was expected to respond independently. In 1998, however, shear strength data obtained from unconfined shear box tests showed that significantly higher strengths could be mobilized across the shear keyed vertical joints between monoliths. Consequently, it was found necessary to re-evaluate the performance of the vertical joints and their influence on the stability of the structure.

The objective of this portion of the assessment was to use the non-linear ANSYS model to determine the magnitude of the forces that would be transferred through the shear keys and be carried into the foundations. With this information it would subsequently be possible to modify the 2-D analyses of each monolith to provide a more realistic assessment of its performance within the 3-D structure.

Based on the linear model described above and shown in Figure 5, non-linear contact elements were incorporated at each vertical joint. The contact surfaces were assigned a friction coefficient  $\mu=1$  and a cohesion of  $c=1$  MPa such that traction normal to the surface would be mobilised at a level consistent with the residual strength observed in unconfined shear box tests. It was not possible to account for the mechanical interlocking of adjacent monoliths with the contact surface elements available in ANSYS. Utilizing the Coulomb friction criterion to approximate the upstream/downstream force transfer between adjacent blocks limits the shear force transfer zone to those areas in contact. However the shape of the shear keys is such that shear could be transferred through the keys outside of the zone identified in the model as carrying cross-valley compressive stresses. Thus the shear stresses obtained in the model are higher than would be the case in the real structure. Consequently, the shear stresses obtained in the model would be higher than those in the real structure.

Vertical loads were considered simultaneously with the horizontal dead and live loads. In order to avoid vertical arching in the model, which due to the sequence of construction would not be present in the real structure, a two-step process was used. In the first step, the gravity load was applied while the friction coefficient was set to zero. This enabled the model to accommodate any differential movement without generating tractions across the contact surface, representing the effect of the concrete placement procedure in the original construction. The second step was to activate the friction in the model and then apply the horizontal loading.

The model was loaded by a constant acceleration around the perimeter of the foundation. Equilibrium was solved for equilibrium as a static load case. Two magnitudes of acceleration were applied to bracket the expected response. The first at 0.56g, corresponded to both the peak of the 5% damped DBE spectrum and also the PGA of the MDE. The second input acceleration at 1.27g corresponded to the peak spectral acceleration of the 5% damped MDE spectrum. Although the upper portions of the dam experience amplifications under dynamic loading conditions, the bulk of the structure is expected to experience base shears less than or equal to that due to the peak of the MDE response spectrum. Thus the two acceleration levels chosen were considered appropriate as they bracket the expected MDE response.

For each of the above load cases, the nodal forces were extracted from each contact surface pair and along the base of each monolith. These nodal forces were summed to give a total force for each location. The results obtained are summarised in Table 4. The maximum stresses distributed across the area of the shear keys, assumed to be 40% of the contact area between monoliths, was found to be 1.96 MPa, within the material capacity. Subsequently it was concluded that the shear keys would not fail in the MDE and the dam would be able to develop 3-D action. The results indicate that the tall, central monoliths (B5, B6 and B7) act to shed their loads to the adjacent monoliths. The monoliths situated on the abutments, however, particularly where the foundation slopes in the cross-valley direction, attract loads shed from the taller monoliths. The two levels of acceleration applied produced similar load sharing ratios. Therefore it was considered appropriate to expect that the load sharing is not load level dependent.

Accounting for the loads shed from the tall monoliths (B6 and B7) enabled the DI team to reverse the prior conclusion that the tall monoliths would be unstable in the MDE. The forces transferred to the abutments, however, would tend to make these monoliths less stable. While the shorter, lighter abutment monoliths have the least capacity to mobilise friction, it has been observed that where the cross-valley slope is significant, some wedging action could take place. Further work is necessary to confirm this beneficial effect; as well as to assess the ability of the shear keys to carry reversed cyclic loading.

**Table 4. Ruskin Dam Block Load Sharing Assessment – MDE – 1.27g peak spectrum Comparison of base shear and total horizontal force.**

Block	Weight (kN)	0.54g Horizontal Force (A) (kN)	0.54g Base Shear (B) (kN)	0.54g (B)/(A) (%)	1.27g Horizontal Force (C) (kN)	1.27g Base Shear (D) (kN)	1.27g (C)/(D) (%)
B1	55158	100085	105422	105%	192607	201948	105%
B2	56937	82737	142787	173%	153463	253547	165%
B3	133446	209955	413238	197%	375428	714826	190%
B4	268671	451492	360304	80%	806014	679240	84%
B5	359859	558694	483519	87%	987056	861172	87%
B6	403897	627641	317601	51%	1110716	577376	52%
B7	335394	532894	295805	56%	938570	618745	66%
B8	147680	232196	677016	292%	420355	1079578	257%

### PIERS AND GATES – HYDRODYNAMIC LOADS

The seismic withstand of the piers and gates contribute significantly to the overall dam safety. The gates and supporting piers are necessary to provide the capacity to control the reservoir in the immediate post-earthquake period. This was found to be necessary to respond to hazardous situations that may develop on the abutments. The upper portions of Ruskin Dam are subjected to high accelerations due to the flexibility of the structure and the associated amplifications of seismic motion. Using Zangar added masses [5], the hydrodynamic loads were found to dominate the seismic loading of the gates.

The Zangar added masses  $m_w(y)$  are given in the following equation for a vertical upstream face:

$$m_w(y) = \frac{C_m}{2} \left[ \frac{y}{H} \left( 2 - \frac{y}{H} \right) + \sqrt{\frac{y}{H} \left( 2 - \frac{y}{H} \right)} \right] \gamma_w H \quad (4)$$

where  $\gamma_w$  is the density of water;  $H$  is the depth of the reservoir,  $y$  is the depth measured down from the reservoir surface, and the coefficient  $C_m = 0.735$  is determined based on numerical data. This mass distribution is derived for the case that the dam moves as a rigid body. A procedure suggested by Kolkman [6], described below, provides a convenient alternative method of establishing hydrodynamic pressures resulting from specified non-uniform velocity or acceleration profiles resulting from a flexible structure.

#### The Kolkman Procedure – 2DOF Dam-Gate Interaction

Kolkman's technique is a simple finite difference scheme that is solved by a relaxation method. The relaxation solution is a simple, iterative numerical procedure that can be easily implemented and solved quickly in a spreadsheet. The values computed correspond to fluid potentials in the reservoir under the assumption that the reservoir behaves as an incompressible, non-viscous fluid. Its simplicity derives from the constraint of setting up a rectilinear grid with equal point spacing in vertical and horizontal directions. Providing that the grid is relatively coarse, convergence times are acceptable given the speed of current PC's.

The fluid potential, once computed, with subsequent processing can be used to determine pressures or added masses. Under the assumption of rigid body motion, the Kolkman technique produces results identical to Zangar and similar to Westergaard, whose solutions consider only the case of rigid body motion of the dam. This suggests that the theoretical basis for the method is sound. When the dam is flexible, however, the Kolkman technique produces different results. In Figure 7, a comparison is made between Kolkman and both Westergaard and Zangar added masses. These results indicate that, near the crest of the dam, the added masses obtained using Kolkman are significantly lower and the forces predicted on the gates and piers at this level are lower than would otherwise be predicted. When amplified motions are taken into account, the Kolkman pressures are approximately half of the corresponding amplified Zangar pressures.

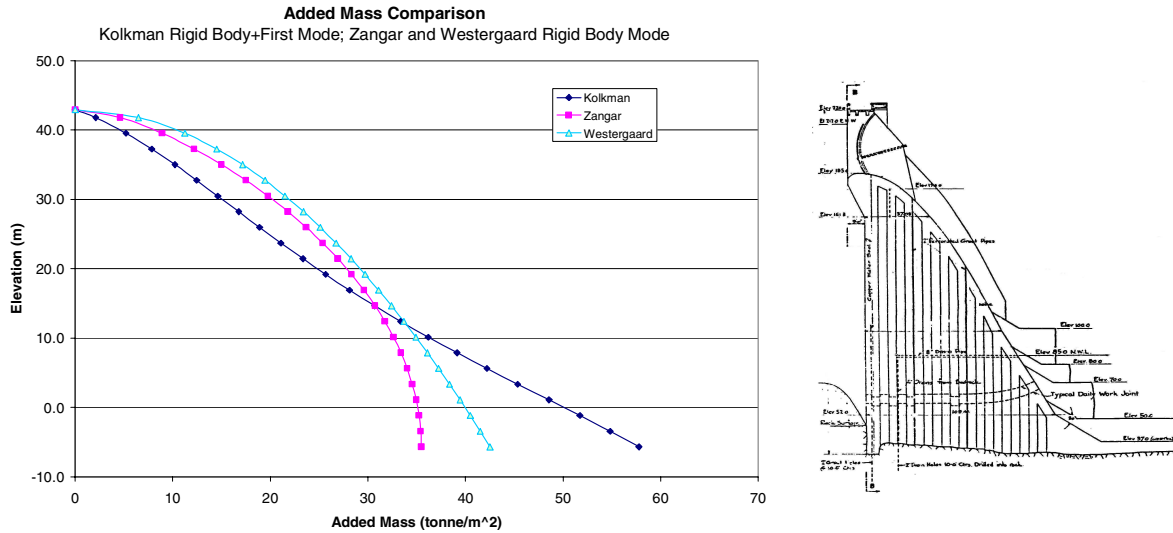


**Figure 7 – Gate 4 added mass Kolkman vs. Westergaard and Zangar**

### 2DOF Dam-Gate Interaction Study

Assuming that the gate is perfectly stiff, the maximum pressures on the gate could be computed using the Kolkman added mass and the amplified accelerations. However, the period of the gate with added mass was computed and it was found to be 7.4 Hz, comparable to that of the dam. Superimposing gate deflections over that of the dam with rigid gate and computing the hydrostatic pressures led to the conclusion that the pressures induced by the flexibility of the gate are not negligible and the interaction between the gate and the dam would need to be assessed. To study the dam-gate interactions a 2DOF modal analysis procedure was devised. The 2DOF dam-gate interaction study was based on the analysis of the 2DOF structure illustrated in Figure 8. The structure contains two components; a single degree of freedom (SDOF) dam model and a SDOF gate model. The SDOF gate model was connected at the top of the dam, as shown.

The mass and stiffness representing the gate was extracted from a detailed finite element study of the gate structure. The lumped mass and stiffness representing the dam was evaluated by first assuming a mode shape for the fundamental vibration mode. Figure 8 illustrates the mode shape,  $\phi_D(h)$  in which the deflection is zero at the base and unity at the crest, assumed to be the point of attachment of the gate. The mass associated with this mode shape is determined as

$$\tilde{m}_D = \int m(h)\alpha^2\phi_D^2(h)dh \quad (7)$$

where  $m(h)$  is the distribution of mass along the height of the dam from the base to the top on the interval  $(0,H)$  and  $\alpha$  is the geometric amplification factor from the base of the dam to the point of attachment of the gate as defined in Figure 8. The associated stiffness is chosen such that the frequency of the model corresponds to the fundamental frequency of vibration of the dam. The correctness of the dam model can be verified by considering a SDOF response spectrum analysis of the dam only. One can thus see that, while the lumped mass will experience the spectral acceleration, the crest of the structure at the point of gate attachment will experience this spectral acceleration multiplied by the geometric amplification factor.

The mass and stiffness matrices of the 2DOF model were determined as follows:

$$M_1 = \begin{bmatrix} \tilde{m}_D + \mu_{DD} & \mu_{DG} \\ \mu_{GD} & m_G + \mu_{GG} \end{bmatrix}; K = \begin{bmatrix} \alpha^2 k_D + \alpha^2 k_G & -\alpha k_G \\ -\alpha k_G & k_G \end{bmatrix} \quad (8)$$

where  $\tilde{m}_D$  is the amplified modal mass of the dam,  $m_G$  is the mass of the gate,  $k_D$  and  $k_G$  are respectively the stiffness of the dam and the gate. The remaining terms,  $\mu_{DD}$ ,  $\mu_{DG}$ ,  $\mu_{GD}$  and  $\mu_{GG}$ , are added mass terms of the reservoir water determined using the Kolkman procedure. In order to evaluate these terms, the acceleration profiles for the case of a unit acceleration of the dam while the gate remains fixed,  $\phi_D(h)$ , and the case of a unit acceleration of the gate while the dam remains fixed,  $\phi_G(h)$  were considered. The pressure distributions resulting from these acceleration profiles are  $p_D(h)$  and  $p_G(h)$ . The added mass terms are computed as follows

$$\mu_{GG} = \int p_G(h)\phi_G(h)dh; \quad \mu_{DG} = \int p_G(h)\phi_D(h)dh; \quad (9)$$

$$\mu_{GD} = \int p_D(h)\phi_G(h)dh; \quad \mu_{DD} = \int p_D(h)\phi_D(h)dh$$

It is interesting to note that the off-diagonal terms do not generally evaluate to the same value.

The mass and stiffness terms defined above have been developed in the relative co-ordinate system. The transformation from relative to absolute co-ordinates, which is necessary to evaluate hydrodynamic loads, is to be taken into account by the inclusion of the rigid body mode in the modal combination. It was identified that the traditional input response spectra provided in Figure 3, yields accelerations of the structure experienced in the absolute co-ordinates. However, this is not consistent with the mode shapes derived based on relative deflections. Therefore, the input spectrum used in the assessment was modified as illustrated in Figure 9. The transformation of the input spectrum was accomplished by using a hyperbolic baseline curve calibrated such that the peak of the response spectrum remained unchanged after transformation.

Once modelled, a modal analysis of the structure was performed and the hydrodynamic pressures corresponding to each mode and the rigid body mode were combined using the SRSS modal combination. Using the transformed spectra, it was confirmed that upon increase of the gate stiffness to an arbitrarily high value, the resulting combined hydrodynamic pressures converged to the rigid gate Kolkman pressures. This was used as an additional check of the procedure. The resulting pressures for the case of the gate having its existing stiffness were found to lie approximately midway between the rigid gate Kolkman pressures and the amplified Zangar pressures.

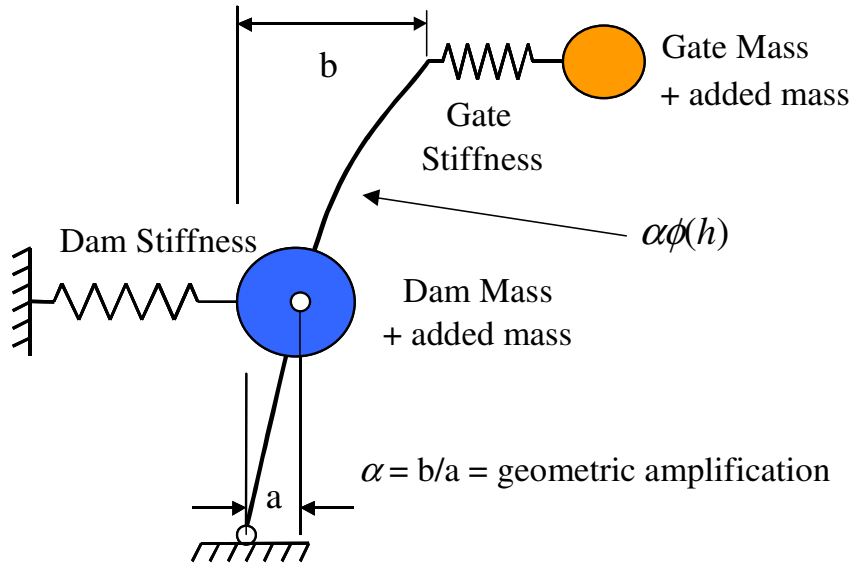


Figure 8 – 2DOF model

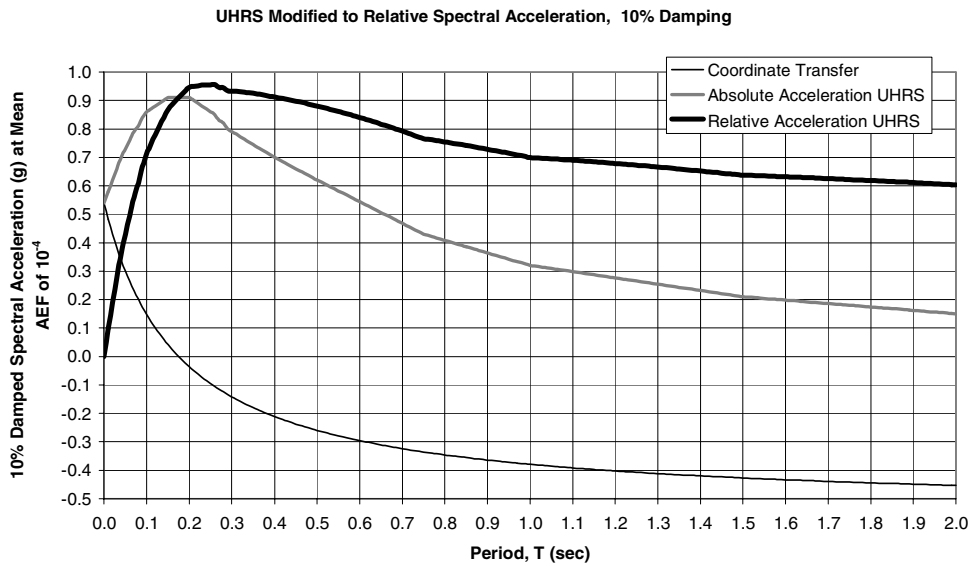


Figure 9 – Modified Uniform Hazard Spectrum

In order to reach a better understanding of the interaction between the dam and the gate, the gate stiffness was varied over a wide range and the hydrodynamic pressures computed. Using these pressures, total gate forces were calculated and plotted against the relative frequency of the dam and the gate as shown in Figure 10. The shape of the curve obtained indicates that the response is near the crest of the interaction curve. This interaction curve provides an understanding of what the response might be if the gate begins to fail and the period lengthens and also whether stiffening of the structure would inadvertently lead to increased forces. For the gate shown, if the period lengthens about 20%, the total force will reach the crest of the interaction diagram, but the total force will still remain below that corresponding to amplified Zangar. Stiffening of the structure would lead to a small reduction in the period ratio and correspondingly a small reduction in the hydrodynamic loads as the force levels approach that corresponding to the rigid gate Kolkman loading.

## CONCLUSIONS AND RECOMMENDATIONS

### Conclusions

1. Performing a combination of analyses as described in this paper, i.e. (1) 3-D linear modal analysis to obtain amplifications at various parts of the dam, (2) 3-D non-linear static analysis to estimate load sharing and (3) detailed 2-D pseudostatic pseudo-dynamic analyses to evaluate seismic stability of individual dam monoliths subjected to the shared loads, is shown to be a practical alternative to the more rigorous but time-history dependant 3-D non-linear dynamic analysis.
2. Based on the lack of suitable North American earthquake recorded time histories it was not possible to support damping of 10-20%. It was concluded that the damping of 5% is appropriate as long as the dam remains elastic.
3. Acceleration data derived from modal analysis in ANSYS gave results relative to the fixed base. However, to provide input for pseudostatic analyses and in particular the determination of hydrodynamic pressures, accelerations in the absolute coordinate system are necessary. These were taken into account by incorporating the rigid-body mode as an additional mode in the modal combination procedure. In order to provide a consistent analysis, the usual input spectra was modified to a relative spectra. At locations where the amplification is high, the correction is negligible.
4. Compared to predictions based on 2-D analyses, 3-D behaviour of the dam causes the tall blocks to shed their loads to the shorter blocks at the abutments. Although the shorter blocks are less able to carry load through friction, cross-valley sloping bases have the potential to mobilize a higher resistance to downstream sliding. This potential beneficial effect needs to be further investigated.
5. A 2-DOF dam-gate interaction analysis was undertaken to provide an improved understanding of the hydrodynamic pressures on the gates. A procedure developed by Kolkman was used to account for varying amplitudes of acceleration in each mode of response of the idealized 2-DOF structure. The resulting hydrodynamic loads on the gates were found to be larger than the loads computed assuming the gates are rigid, but less than those determined using the amplified Zangar approach.

### Recommendations

1. Further research is recommended to identify the appropriate levels of damping to be used in the assessment of the earthquake response of the dam-foundation-reservoir system.
2. It is recommended to investigate the contribution of cross-valley sloping dam/foundation interfaces to the available shear strength when the abutment dam blocks are confined
3. Experimental work is recommended to confirm the hydrodynamic loads obtained using of the 2-D dam-gate interaction study methodology.

## ACKNOWLEDGEMENTS

The authors gratefully acknowledge the Director of Dam Safety, BC Hydro, for sponsoring the Ruskin Dam deficiency investigation work and permitting its use as the case study for this paper. The authors also acknowledge the valuable input from Dr. C.E. Ventura and the contribution by partnership student J. Yoneda of the University of British Columbia in carrying out much of the analysis reported in this paper.

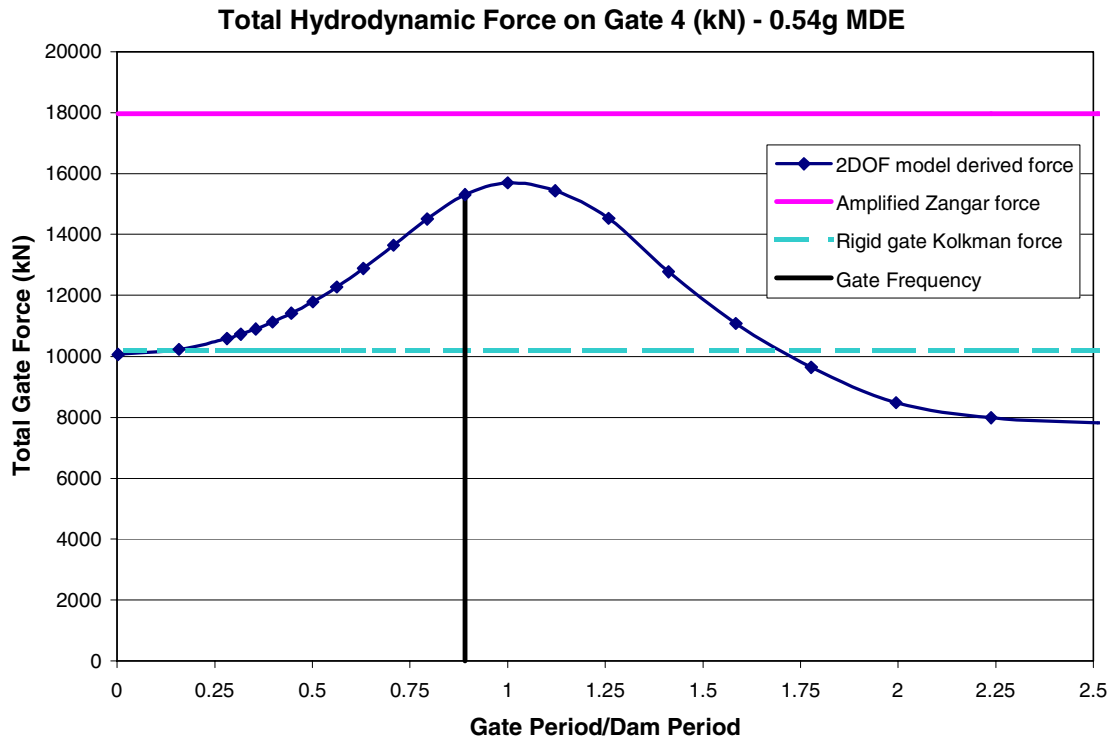


**Figure 10 – Gate 4 force vs. gate period.**

### REFERENCES

1. Chopra, A.K. and Tan, H. "Simplified Earthquake Analysis of Gated Spillway Monoliths of Concrete Gravity Dams." US Army Corps of Engineers Structures Laboratory, Waterways Experimental Station, Technical Report SL-89-4, March 1989.
2. Okamoto, Shunzo, Introduction to Earthquake Engineering, John Wiley and Sons, 1973.
3. Hall, J.F. "The dynamic and earthquake behavior of concrete dams: review of experimental behavior and observational evidence." Soil Dynamics and Earthquake Engineering, Vol. 7, No. 2, April 1988.
4. Kemp, B.G., Ventura, C.E., Anderson, D.L. and Felber, A.J., "Ambient Vibration Measurement of Ruskin Dam for Seismic Assessment", Seventh Canadian Conference on Earthquake Engineering, 1995
5. Zangar, C.N. "Hydrodynamic Pressures on Dams due to Horizontal Earthquakes," Proceedings of the Annual Meeting of the Society for Experimental Stress Analysis, Vol. X, No. 2, pp. 93-102.
6. Kolkman, P.A. "A simple scheme for calculating added mass of hydraulic gates," Journal of Fluids and Structures, Vol. 2 pp.339-353, 1988